

# Detection of pesticides on navel orange skin by surface-enhanced Raman spectroscopy coupled with Ag nanostructures

Liu Yande\*, Zhang Yuxiang, Wang Haiyang, Ye Bing

(Institute of Optics-Mechanics-Electronics Technology and Application, East China Jiaotong University, Nanchang 330013, China)

**Abstract:** Residual pesticides such as phosmet and chlorpyrifos in fruit have become a public concern problem in recent years. In this study, surface-enhanced Raman spectroscopy (SERS) was used to detect and characterize pesticides extracted from navel orange surfaces. Silver colloid was prepared for getting the SERS of phosmet and chlorpyrifos. Enhanced Raman signals of phosmet over a concentration range of 5 mg/L to 30 mg/L and chlorpyrifos over a concentration range of 5 mg/L to 20 mg/L were acquired. Partial least squares (PLS) regression combined with different data preprocessing methods was used to develop quantitative models. With the second derivative data preprocessing, the best prediction model of phosmet pesticide was achieved with a correlation coefficient ( $r$ ) of 0.852 and the root mean square error of prediction (RMSEP) of 5.177 mg/L. The best prediction model of chlorpyrifos pesticide was achieved with  $r$  of 0.843 and the RMSEP of 2.992 mg/L using the multiplicative scatter correction (MSC) and first derivative data preprocessing. This study indicated that SERS coupled with Ag nanostructures is a potential tool for analysis of phosmet and chlorpyrifos pesticide residues.

**Keywords:** pesticides residues, detection, silver colloid, surface enhanced Raman spectroscopy, navel orange, food safety

**DOI:** 10.3965/j.ijabe.20160902.1960

**Citation:** Liu Y D, Zhang Y X, Wang H Y, Ye B. Detection of pesticides on navel orange skin by surface-enhanced Raman spectroscopy coupled with Ag nanostructures. Int J Agric & Biol Eng, 2016; 9(2): 179–185.

## 1 Introduction

In agricultural fields, application of organophosphorus pesticides (OPPs) has become a major method in pest control throughout the world. OPPs are considered to have potent neurotoxicity. They have the ability of inactivating acetylcholinesterase<sup>[1,2]</sup>. These enzymes remove acetylcholine, leading to rapid twitching of voluntary muscles and finally paralysis or heart failure<sup>[3]</sup>. According to Residue Monitoring Reports published by the US Food and Drugs Administration (US FDA),

pesticide residues exist in a large portion of certain types of fruits<sup>[4]</sup>. The organophosphates kill insects by attacking the central nervous system and also pose a threat to human health. Therefore, effective methods to detect OPPs are urgently needed.

The analysis methods used to detect the residual pesticides on the surface of fruits include thin-layer chromatography<sup>[5]</sup>, gas chromatography<sup>[6]</sup> and high performance liquid chromatography<sup>[7]</sup>. In recent years, some new analytical methods for detection of fruit pesticides have been reported, including fluorescence polarization immunoassay<sup>[8]</sup>, liquid chromatography-mass spectrometry<sup>[9-11]</sup>, multi-enzyme inhibition assay<sup>[12]</sup> and biosensors<sup>[13]</sup>. However, these methods are time consuming, labor intensive, and often require complicated procedures of sample preparation.

Raman spectroscopy has long been considered a useful analytical technique to evaluate food safety and quality<sup>[14]</sup>. Some types of pesticides have been detected

**Received date:** 2015-05-19    **Accepted date:** 2015-10-26

**Biographies:** **Zhang Yuxiang**, Master student, Majoring in spectroscopy detection, Email: 13047917899@163.com; **Wang Haiyang**, Master, Majoring in optics-mechanics-electronics technology and application, Email: wanghaiyangjl1988@163.com; **Ye Bing**, Master, Majoring in spectroscopy detection, Email: 348961311@qq.com.

**\*Corresponding author:** **Liu Yande**, PhD, Professor, Majoring in optics-mechanics-electronics technology and application, Tel: +86-791-87046173, Email: jxliuyd@163.com.

by Raman spectroscopy, such as cypermethrin<sup>[15]</sup>, iprodione<sup>[16]</sup>, cyromazine<sup>[17]</sup>, diazinon<sup>[18]</sup>, and fenthion<sup>[19]</sup>. Because of its high accuracy and sensitivity, the SERS (surface-enhanced Raman scattering) technique has already been applied for detection of organophosphate and carbamate pesticides, including detection of organophosphate and carbamate pesticides in fruit with gold nanostructures<sup>[20]</sup>, quantitative detection of carbary pesticides with Ag nanoparticles-coated Si nanowire arrays<sup>[21]</sup>, analysis of fonofos pesticide on silver and gold nanoparticles<sup>[22]</sup>, study of the absorption of the insecticide cyromazine on Ag colloid<sup>[23]</sup>, analysis of the adsorption of dimethoate and omethoate on Ag hydrosols<sup>[24]</sup>, and the surface enhanced Raman scattering spectra of dimethoate at different concentrations with different acidic and basic conditions<sup>[25]</sup>.

According to Wang et al.<sup>[26]</sup>, AuNPs decorated glycidyl methacrylate-ethylene dimethacrylate (GMA-EDMA) powder material served as the solid-phase extraction (SPE) sorbent is synthesized. With this method, SERS spectra of phosmet and disulfoton could be identified at concentrations of 5 µg/L and 1 µg/L, respectively. Dhakal et al.<sup>[27]</sup> explored the application of Raman spectroscopy for detection of chlorpyrifos pesticide in apple surface. It shows that the developed system can detect chlorpyrifos residue to minimum limit of 6.69 mg/kg. Zhang et al.<sup>[28]</sup> developed a novel SERS substrate using gold nanorods and SERS can detect as low as 0.1 ppm of carbaryl.

In principle, the signal intensity observed in spontaneous SERS measurements is proportional to the concentration in the probed volume, so it should be possible to make a direct calibration plot of the absolute intensity of the Raman band against concentration. The objective of this study was to detect and characterize phosmet and chlorpyrifos pesticides extracted from navel orange surfaces using a SERS spectroscopic technique coupled with Ag nanostructures.

## 2 Materials and methods

### 2.1 Materials

Phosmet and chlorpyrifos pesticides were purchased from AccuStandard, Inc. (New Haven, CT 06513). Navel

oranges were purchased directly from the fruit store, and were cleaned to ensure that no pesticide residues existed on the samples.

### 2.2 Sample solutions preparation

Phosmet and chlorpyrifos were diluted into a 5000 mg/L solution using a mixed solvent system (methanol/H<sub>2</sub>O=1:1, v/v). The cleaned navel orange skin was cut into five small square pieces (2 mm×2 mm), and 0.5 mL of pesticide solution was added on each surfaces. After pesticides on the navel orange skin was allowed to air-dry, the skin was broken into many small pieces, added to an acetonitrile solution, and then stirred for about 40 min. Pesticides on the navel orange skin dissolve in acetonitrile solution. Then filter papers were used to separate the acetonitrile solution and the small skin pieces. Filtrate was diluted to 50 mg/L. The phosmet concentration ranged from 5 mg/L to 30 mg/L (26 different concentrations) at 1 mg/L interval and the chlorpyrifos concentration ranged from 5 mg/L to 20 mg/L (31 different concentrations) at 0.5 mg/L interval.

The 50 mg/L solution of phosmet and chlorpyrifos were sent to the Center of Analysis and Testing at Nanchang University. The real concentration of phosmet detected by gas chromatography was 12.3 mg/L, and the actual recovery of the phosmet was 24.6%. The real concentration of phosmet detected by gas chromatography was 12.6 mg/L, and the actual recovery of the phosmet was 25.2%. So the 5 mg/L solution of phosmet and chlorpyrifos was actually 1.23 mg/L and 1.26 mg/L, respectively.

### 2.3 SERS instrumentation and acquisition

Silver colloid for SERS measurements was prepared by means of the Lee method<sup>[29]</sup>. The samples were prepared by adding 200 µL of aqueous analytes, 40 µL of silver colloid, 60 µL of a 160 mmol/L NaCl solution. After 10 min of homogeneous mixing, a 2 µL sample was placed on a quartz plate. A confocal micro-Raman spectrometer (Bruker, Senterra) equipped with a CCD detector (thermo-electrically cooled, 1025×256 pixels) was used to collect the Raman spectra and SERS spectra. This system is equipped with a 785 nm laser source. The laser power reaching the sample was about 10 mW and a 20× microscope objective was used for all spectral

acquisitions. All spectral data were collected by Opus 6.5 software (Bruker) with a resolution of  $9\text{ cm}^{-1}$ . The exposure time was 5 s per scan and each spectrum was the average of three scans.

### 3 Results and discussion

#### 3.1 Raman spectra of Phosmet and chlorpyrifos

The chemical structures of phosmet and chlorpyrifos are shown in Figure 1. The two pesticides have common chemical bond of P=S. Raman spectra of the phosmet and chlorpyrifos in solid form were obtained, and are shown in Figure 2. The spectra of phosmet and chlorpyrifos exhibit the most prominent peaks at around  $651\text{ cm}^{-1}$  due to the in-plane deformation vibration of P=S. The band assignments summarized in Table 1 are based on other published data<sup>[30]</sup>. Although phosmet and chlorpyrifos have similar Raman spectral features, each pesticide has a unique molecular structure.

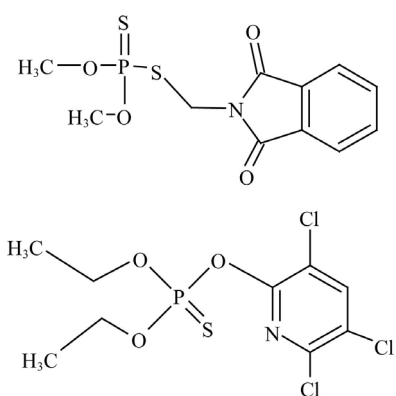


Figure 1 Chemical structures of phosmet (upper) and chlorpyrifos (bottom)

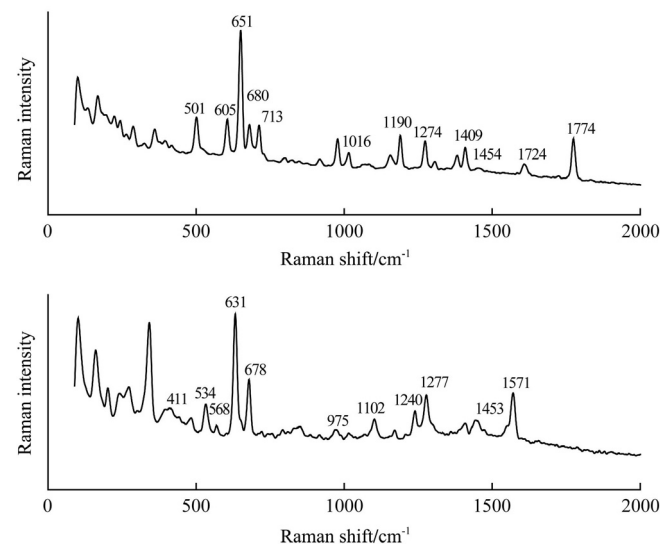


Figure 2 Raman spectra of solid phosmet (top) and chlorpyrifos

**Table 1 Band assignments of major peak in Raman spectra acquired from two pesticides**

Band/cm <sup>-1</sup>	Assignment
Phosmet	
605	C=O in-plane deformation
651	P=S in-plane deformation
680	P=S stretch
713	Benzene ring breathing
1016	P—O—C deformation
1190	P—O—CH <sub>3</sub> out-of plane deformation
1274	C—N stretch
1409	C—H out-of plane deformation
1454	C—H deformation
1724	C=O stretch
Chlorpyrifos	
411	C—Cl stretch
534	P—O stretch
568	P=S or C—Cl stretch
631	P=S or C—Cl stretch
678	C—Cl stretch
975	P—O—C stretch
1102	P—O—C stretch
1240	Ring mode
1277	Ring mode
1453	C—H deformation
1571	Ring stretching mode

#### 3.2 SERS spectra of phosmet and chlorpyrifos

The SERS spectra of different concentrations of phosmet and chlorpyrifos pesticides solutions extracted from Navel orange skin are shown in Figures 3, 4. The relative intensity of the SERS spectra of pesticide bands differed from that of its spontaneous Raman spectrum. Meanwhile, as the blank spectrum of the extracted orange peels, the SERS spectra of the solution without any pesticides are shown in Figure 5. The peaks of the blank spectrum are different from the peaks of the pesticides. Interactions between analytical molecules and substrate surface should be taken into account for the enhancement of Raman scattering signals, which induces the SERS apart from spontaneous Raman spectroscopy.

Comparing the Raman spectra of solid pesticides and the SERS spectra of pesticides solutions, some peaks appeared in the spontaneous Raman spectrum could be downshifted, upshifted, or disappeared in the SERS spectrum. For example, the peaks at  $501\text{ cm}^{-1}$ ,  $605\text{ cm}^{-1}$  and  $1016\text{ cm}^{-1}$  in the normal Raman spectrum of phosmet were upshifted to  $505\text{ cm}^{-1}$ ,  $614\text{ cm}^{-1}$  and  $1017\text{ cm}^{-1}$  in the SERS spectrum, the peak at  $1454\text{ cm}^{-1}$  in the Raman spectrum of phosmet was downshifted to  $1450\text{ cm}^{-1}$  in the

SERS spectrum. The peak at  $1278\text{ cm}^{-1}$  and  $1571\text{ cm}^{-1}$  in the normal Raman spectrum of chlorpyrifos were downshifted to  $1272\text{ cm}^{-1}$  and  $1567\text{ cm}^{-1}$  in the SERS spectrum, and the peak at  $1444\text{ cm}^{-1}$  in the normal Raman spectrum of chlorpyrifos was upshifted to  $1451\text{ cm}^{-1}$  in the SERS spectrum.

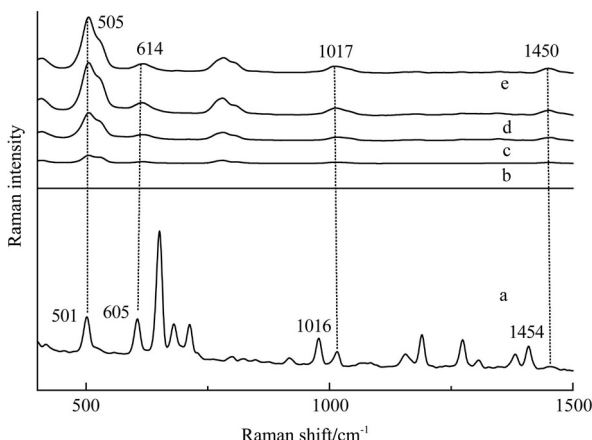


Figure 3 Raman spectra of (a) solid phosmet and SERS spectra of phosmet solutions concentrations, (b) 5 mg/L, (c) 10 mg/L, (d) 20 mg/L and (e) 30 mg/L

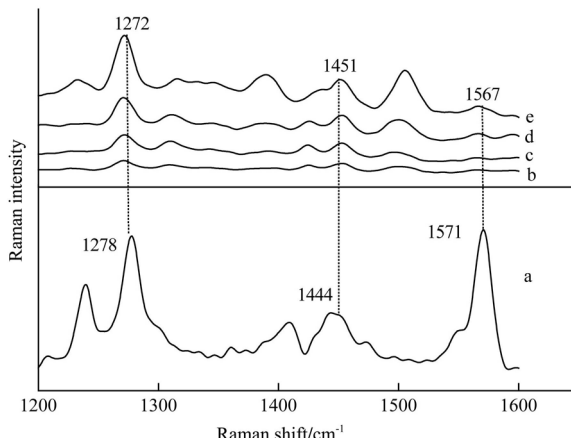


Figure 4 Raman spectra of (a) solid chlorpyrifos and SERS spectra of chlorpyrifos solutions concentrations, (b) 5 mg/L, (c) 10 mg/L, (d) 15mg/L and (e) 20 mg/L

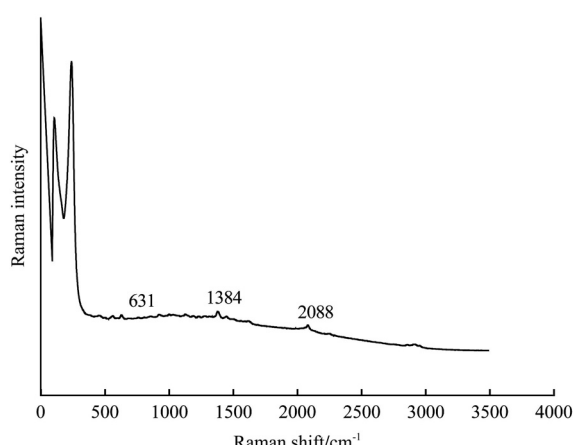


Figure 5 SERS spectra of solution without any pesticides

Figures 3, 4 show the SERS spectra of phosmet and chlorpyrifos at different concentrations, respectively. For phosmet, the characteristic peaks at around  $505\text{ cm}^{-1}$  and  $614\text{ cm}^{-1}$  could be discerned at concentrations as low as 5 mg/L, although the other two characteristic peaks at around  $1017\text{ cm}^{-1}$  and  $1050\text{ cm}^{-1}$  were very weak. The peaks at  $1272\text{ cm}^{-1}$  and  $1451\text{ cm}^{-1}$  for chlorpyrifos also could be discerned at the 5 mg/L level. In general, the intensity of some prominent peaks increased with an increase of pesticide concentration, although the increase rate varied for different absorption bands.

### 3.3 Quantitative analysis

The detection limit (DL) with the 99.86% confidence interval can be calculated from the PLS calibration curve based on characteristic peaks in SERS spectra using the following formula<sup>[31]</sup>:

$$\text{MDL} = 3\sigma/m \quad (1)$$

where,  $\sigma$  is the standard error of predicted concentration, and  $m$  is the slope of the calibration curve. In a PLS model,  $\sigma$  equals to RMSEP<sup>[32]</sup>.

The SERS spectra acquired from the pesticide samples were used to analyze the detection limits for the phosmet and chlorpyrifos residues extracted from the navel orange skin. Detection limits for the pesticides were calculated by Equation (1). Figures 6 and 7 show the calibration curves of phosmet and chlorpyrifos, respectively. Results of the detection limits for the two pesticides are summarized in Table 2.

A chemometric method was used to correlate the actual value of pesticide with the SERS spectral data acquired through silver colloid. A PLS analysis model was applied on spectra of the two pesticide samples and the result of the calibration model was evaluated by minimizing root mean square error of cross-validation (RMSECV), the root mean square error of prediction (RMSEP), and the correlation coefficient ( $r$ ). A good model should have the lower RMSECV, RMSEP and the higher  $r$ , but also a small difference between RMSECV and RMSEP. In addition, the number of factors should be as few as possible, because a large number may include some irrelevant information.

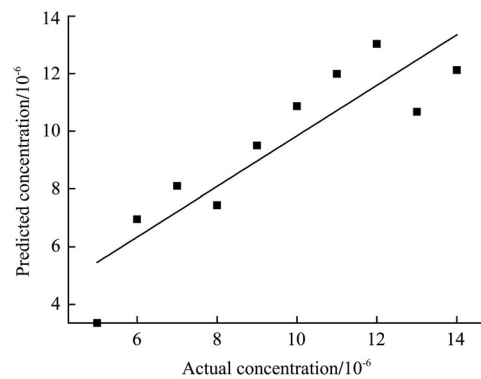


Figure 6 Calibration curve of phosmet using the PLS models

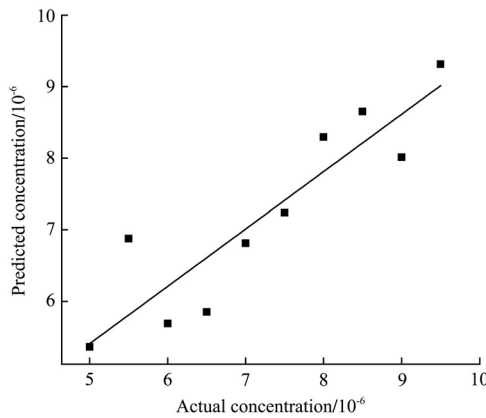


Figure 7 Calibration curve of chlorpyrifos using PLS models

**Table 2 Calculation of detection limits (DL) of SERS method for phosmet and chlorpyrifos extracted from navel orange skin**

	Standard error	Slope	DL/mg·L <sup>-1</sup>
Phosmet	1.309	0.876	4.483
Chlorpyrifos	0.800	0.614	3.909

Table 3 shows the results of the calibration models obtained by PLS regression with different preprocessing methods for determining phosmet pesticide. SERS spectral data of phosmet were preprocessed with six types of preprocessing methods in the region from 90 cm<sup>-1</sup> to 3500 cm<sup>-1</sup>. The best prediction model of phosmet pesticide was achieved with a correlation coefficient of 0.852 and RMSEP of 5.177 mg/L, with the second derivative data preprocessing. The PLS model predicted values of phosmet concentrations are shown in Table 4.

Table 5 shows the results of different preprocessing methods for determining chlorpyrifos pesticide. SERS spectral data of chlorpyrifos were preprocessed with five types of preprocessing methods in the region from 90 to 3500 cm<sup>-1</sup>. The best prediction model of chlorpyrifos pesticide was achieved with a correlation coefficient of 0.843 and RMSEP of 2.992 mg/L, with the MSC and first derivative data preprocessing. The PLS model predicted

values of chlorpyrifos concentrations are shown in Table 6.

**Table 3 Comparison results for phosmet solution concentrations developed by PLS with different preprocessing methods**

Preprocessing method	Factors	Calibration Set		Prediction Set	
		$R_C$	RMSECV/mg·L <sup>-1</sup>	$R_P$	RMSEP/mg·L <sup>-1</sup>
Origin	3	0.959	2.056	0.796	5.364
1 <sup>st</sup> D	4	0.981	1.403	0.827	5.351
2 <sup>nd</sup> D	1	<b>0.897</b>	<b>3.212</b>	<b>0.852</b>	<b>5.177</b>
SNV	6	0.913	2.963	0.815	5.049
MSC	5	0.893	3.277	0.808	5.092
1 <sup>st</sup> + SNV	4	0.930	2.682	0.781	5.420
1 <sup>st</sup> + MSC	4	0.914	2.949	0.708	7.367

Note: 1<sup>st</sup> D-first derivative; 2<sup>nd</sup> D-second derivative; SNV-standard normal variate; MSC-multiplicative scatter correction.

**Table 4 Relationship of predicted concentrations with the reference values of phosmet solutions by PLS with 2<sup>nd</sup> D**

Actual concentration/mg·L <sup>-1</sup>	Predicted concentration/mg·L <sup>-1</sup>
6	10.476
9	12.093
12	9.105
15	13.213
18	16.5
22	21.984
27	16.735
30	21.902

**Table 5 Comparison results for chlorpyrifos solution concentrations developed by PLS with different preprocessing methods**

Preprocessing method	Factors	Calibration Set		Prediction Set	
		$R_C$	RMSECV/mg·L <sup>-1</sup>	$R_P$	RMSEP/mg·L <sup>-1</sup>
Origin	5	0.851	2.404	0.681	3.207
1 <sup>st</sup> D	2	0.716	3.198	0.704	3.404
SNV	3	0.810	2.687	0.705	3.355
MSC	1	0.787	2.825	0.516	3.794
SNV+1 <sup>st</sup>	4	0.928	1.704	0.764	2.983
MSC+1 <sup>st</sup>	5	<b>0.950</b>	<b>1.434</b>	<b>0.843</b>	<b>2.992</b>

**Table 6 Relationship of predicted concentrations with the reference values of chlorpyrifos solutions by PLS with MSC and 1<sup>st</sup> D**

Actual concentration/mg·L <sup>-1</sup>	Predicted concentration/mg·L <sup>-1</sup>
6.0	5.066
7.5	9.778
9.0	8.423
10.5	11.375
12.0	10.428
14.0	9.525
15.5	15.507
16.5	11.934
18.0	12.965
19.5	15.807

## 4 Conclusions

The results of this study showed that phosmet and chlorpyrifos could be detected at concentration levels as low as 1.23 mg/L and 1.26 mg/L using SERS coupled with silver colloid. Pesticide residues on naval orange skin can be rapidly extracted and detected by SERS. Although the  $r$  values 0.852 and 0.843 for PLS models for the tested pesticides were not very optimistic results, a quantitative method for detecting pesticide residues will have great promise with further development of SERS substrates and the aid of chemometric methods.

## Acknowledgments

The authors gratefully acknowledge the financial support provided by the National Science and Technology Support Program (31160250, 61178036).

## [References]

- [1] Costa L G. Current issues in organophosphate toxicology. *Clinica Chimica Acta; International Journal of Clinical Chemistry*, 2006; 366(1-2): 1–13.
- [2] Gupta R C. Brain regional heterogeneity and toxicological mechanisms of organophosphates and carbamates. *Toxicology Mechanisms & Methods*, 2004; 14(3): 103–143.
- [3] Kamrin M A. *Pesticide Profiles: Toxicity, Environmental Impact, and Fate*. CRC Press: Boca Raton, 1997.
- [4] FDA. Pesticide monitoring program fy 2007.
- [5] Kar A, Mandal K, Singh B. Decontamination of Chlorantraniliprole Residues on Cabbage and Cauliflower through Household Processing Methods. *Bulletin of Environmental Contamination & Toxicology*, 2012; 88(4): 501–506.
- [6] Wu J, Liu Y, Zhao R, Xu R. Fast pesticide multiresidue analysis in American ginseng (*Panax quinquefolium* L.) by gas chromatography with electron capture detection. *Journal of Natural Medicines*, 2011; 65(2): 406–409.
- [7] Seebunrueng K, Santaladchaiyakit Y, Soisungnoen P, Srijaranai S. Cationic surfactant ambient cloud point extraction and high-performance liquid chromatography for simultaneous analysis of organophosphorus pesticide residues in water and fruit juice samples. *Analytical & Bioanalytical Chemistry*, 2011; 401(5): 1703–1712.
- [8] Kolosova A Y, Park J H, Eremin S A, Kang S J, Chung D H. Fluorescence polarization immunoassay based on a monoclonal antibody for the detection of the organophosphorus pesticide parathion-methyl. *J. Agric. Food Chem*, 2003; 51(5): 1107–1114.
- [9] Grimalt S, Pozo Ó J, Sancho J V, Hernández F. Use of liquid chromatography coupled to quadrupole time-of-flight mass spectrometry to investigate pesticide residues in fruits. *Analytical Chemistry*, 2007; 79(7): 2833–2843.
- [10] Liu M, Hashi Y, Song Y, Lin J M. Simultaneous determination of carbamate and organophosphorus pesticides in fruits and vegetables by liquid chromatography–mass spectrometry. *Journal of chromatography A*, 2005; 1097(1), 183–187.
- [11] Ortelli D, Edder P, Corvi C. Pesticide residues survey in citrus fruits. *Food Additives & Contaminants*, 2005; 22(5): 423–428.
- [12] Ingrid W, Wolfgang S. Multienzyme inhibition assay for residue analysis of insecticidal organophosphates and carbamates. *Journal of Agricultural & Food Chemistry*, 2007; 55(26): 10563–10571.
- [13] Valdés-Ramírez G, Fournier D, Ramírez-Silva M T, Marty J L. Sensitive amperometric biosensor for dichlorovos quantification: Application to detection of residues on apple skin. *Talanta*, 2008; 74(4): 741–746.
- [14] Lu X, Al-Qadiri H M, Lin M, Rasco B A. Application of Mid-infrared and Raman Spectroscopy to the Study of Bacteria. *Food & Bioprocess Technology*, 2011; 4(6): 919–935.
- [15] Zhang P X, Zhou X, Cheng A Y, Fang Y. Raman Spectra from Pesticides on the Surface of Fruits. *Journal of Physics Conference Series*, 2006; 7–11.
- [16] Armenta S, Garrigues S, Guardia M D L. Determination of iprodione in agrochemicals by infrared and Raman spectrometry. *Analytical & Bioanalytical Chemistry*, 2007; 387(8): 2887–2894.
- [17] Armenta S, Quintás G, Garrigues S, de la Guardia M. Determination of cyromazine in pesticide commercial formulations by vibrational spectrometric procedures. *Analytica Chimica Acta*, 2004; 524(1): 257–264.
- [18] Skoulika S G, Georgiou C A, Polissiou M G. FT-Raman spectroscopy - analytical tool for routine analysis of diazinon pesticide formulations. *Talanta*, 2000; 51(3): 599–604.
- [19] Skoulika S G, Georgiou C A, Polissiou M G. Quantitative Determination of Fenthion in Pesticide Formulations by FT-Raman Spectroscopy. *Applied Spectroscopy*, 1999; 53: 1470–1474.
- [20] Liu B, Zhou P, Liu X, Sun X, Li H, Lin M. Detection of pesticides in fruits by surface-enhanced raman spectroscopy coupled with gold nanostructures. *Food Bioprocess Tech*, 2013; 6(3): 710–718.
- [21] Wang X T, Shi W S, She G W, Mu L X, Lee S T. High-performance surface-enhanced Raman scattering

- sensors based on ag nanoparticles-coated Si nanowire arrays for quantitative detection of pesticides. *Applied Physics Letters*, 2010; 96: 053104–053104.
- [22] Jitraporn V, Robertson E G, Don M N. Surface - enhanced Raman spectroscopic analysis of fonofos pesticide adsorbed on silver and gold nanoparticles. *Journal of Raman Spectroscopy*, 2010; 41(10): 1137–1148.
- [23] Mukherjee K, Sanchez-Cortes S, Garcia-Ramos J V. Raman and surface-enhanced Raman study of insecticide cyromazine. *Vibrational Spectroscopy*, 2001; 25(1): 91–99.
- [24] [24] Guerrini L, Sanchez-Cortes S, Cruz V L, Martinez S, Ristori, S, Feis A. Surface - enhanced Raman spectra of dimethoate and omethoate. *Journal of Raman Spectroscopy*, 2011; 42(5): 980–985.
- [25] He Q, Li S, Guenter S. The study of dimethoate by means of vibrational and surface enhanced Raman spectroscopy on Au/Ag core-shell nanoparticles. *Spectroscopy and Spectral Analysis*, 2010; 30(12): 3249–3253.
- [26] Wang X, Du Y, Zhang H, Xu Y, Pan Y, Wu T, Hu H. Fast enrichment and ultrasensitive in-situ detection of pesticide residues on oranges with surface-enhanced Raman spectroscopy based on Au nanoparticles decorated glycidyl methacrylate–ethylene dimethacrylate material. *Food Control*; 2014; 46: 108–114.
- [27] Dhakal S, Li Y, Peng Y, Chao K, Qin J, Guo L. Prototype instrument development for non-destructive detection of pesticide residue in apple surface using Raman technology. *Journal of Food Engineering*, 2014; 123(2): 94–103.
- [28] Zhang Z, Yu Q, Li H, Mustapha A, Lin M.. Standing Gold Nanorod Arrays as Reproducible SERS Substrates for Measurement of Pesticides in Apple Juice and Vegetables. *Journal of Food Science*, 2015; 80(2): N450–N458.
- [29] Lee P C, Meisel D J. Adsorption and Surface-Enhanced Raman of Dyes on Silver and Gold Sols. *Journal of Physical Chemistry*, 1982; 86(17): 3391–3395.
- [30] Shende C, Inscore F, Sengupta A, Stuart J, Farquharson S. Rapid extraction and detection of trace chlorpyrifos-methyl in orange juice by surface-enhanced Raman spectroscopy. *Sensing and Instrumentation for Food Quality and Safety*, 2010; 4(3-4): 101–107.
- [31] Strickland A D, Batt C A. Detection of carbendazim by surface-enhanced Raman scattering using cyclodextrin inclusion complexes on gold nanorods. *Analytical Chemistry*, 2009; 81(8): 2895–2903.
- [32] Liu B, Zhou P, Liu X, Sun X, Li H, Lin M. Detection of Pesticides in Fruits by Surface-Enhanced Raman Spectroscopy Coupled with Gold Nanostructures. *Food & Bioprocess Technology*, 2013; 6(3): 710–718.